



A review of radiation effects on ceramic wasteform alteration

Neil Hyatt*

Department of Materials Science & Engineering,
University of Sheffield, UK

ICTP Summer School on Radiation Effects on Nuclear Wasteforms
11-16 September 2016

*The views expressed in this talk are the personal opinion of the speaker
and do not necessarily reflect those of sponsors or funding agencies*



University of Sheffield

Research Capability

- Largest UK academic research group working on radioactive waste management & disposal
- 7 academic staff
- 18 Postdoctoral Research Associates
- ca. 40 PhD students
- ca. 20 MSc / MEng and visiting staff, typically
- Research order book of £10m+
- Also strong capability underpinning nuclear materials: metallurgy, manufacturing, fusion.

Facilities

- £4M UoS / DECC investment in radio-materials and radio-chemistry laboratories
- Unique for Tc / TRU materials science in neg. pressure glove boxes in UK academic sector





Synchrotron micro-focus X-ray studies

Synchrotron X-ray spectroscopy applied to environmental contaminants

Provides unique insight into materials alteration by spectroscopy and diffraction

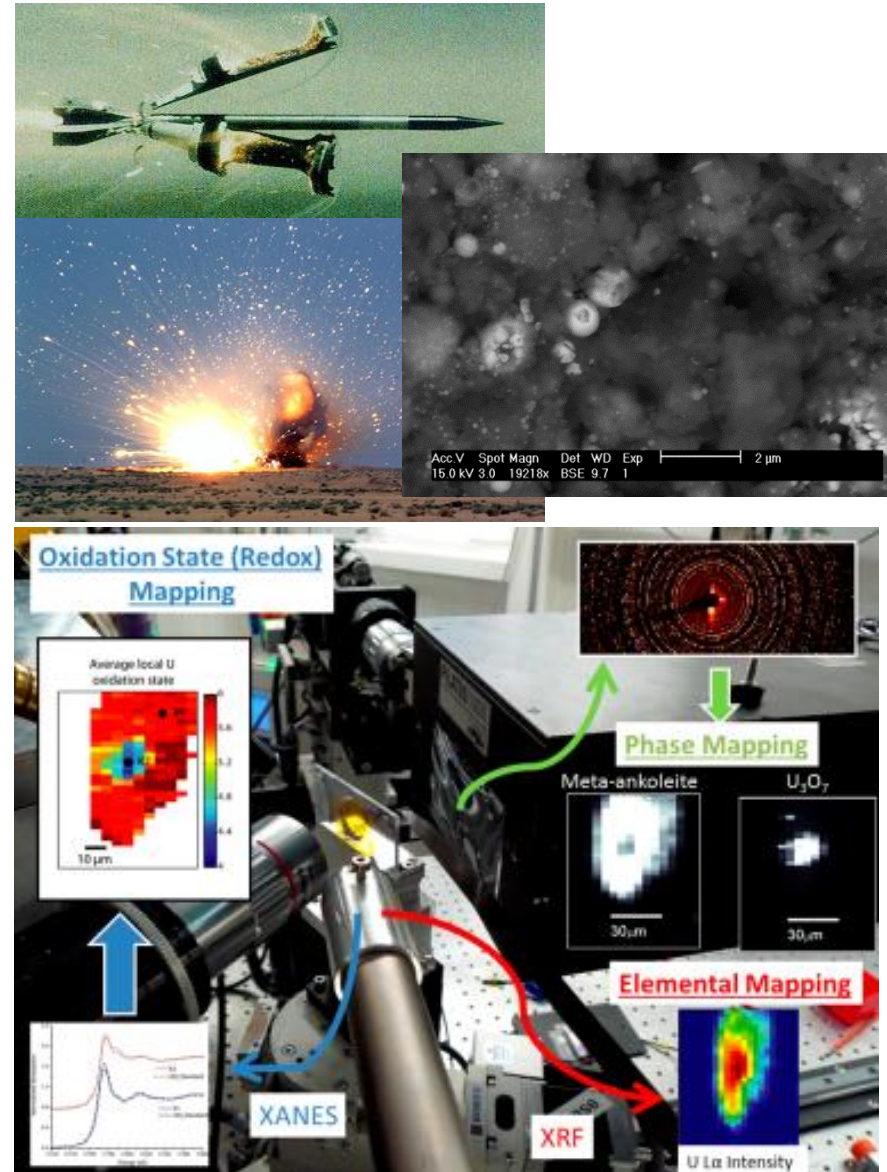
Example – MOD Eskmeals; DU contamination from munitions testing

Particulates weathered for more than 30y in wet oxic surface environment

Evidence for formation and stability of ternary U(V) phases

[Crean et al., J. Haz. Mat., 263 \(2013\) 382](#)

[Crean et al., Env. Sci. Tech., 48 \(2014\) 1467](#)





Decommissioning Fukushima NPP

Ion exchange materials utilised to decontaminate water from reactor complex

In-flow of groundwater $>150\text{m}^3$ per day and $>720\text{m}^3$ of water treated per day

Ion exchange materials are self heating require conditioning:

- Water radiolysis – H_2 generation
- Self dessication
- Radiation and chloride aggravated stress-corrosion cracking

Conversion of granular inorganic ion exchange materials to passively safe ceramic by Hot Isostatic Pressing

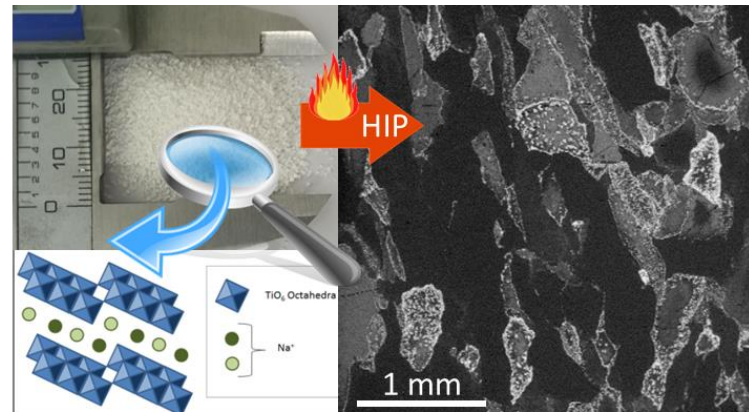


Figure 1. Sr Treat granules with layered titanate structure ($\text{Na}_2\text{Ti}_6\text{O}_{13}$), transformed into dense ceramic wasteform as shown by back scattered SEM. Bright areas correspond to Sr rich phases, the inhomogeneous Sr distribution reflects the different Sr uptake during ion exchange.

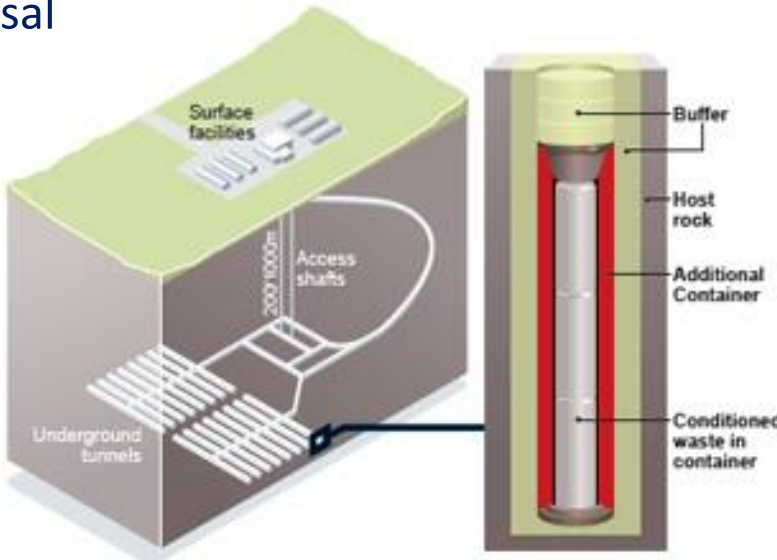


Does radiation damage impact the long term durability of ceramic wasteforms?



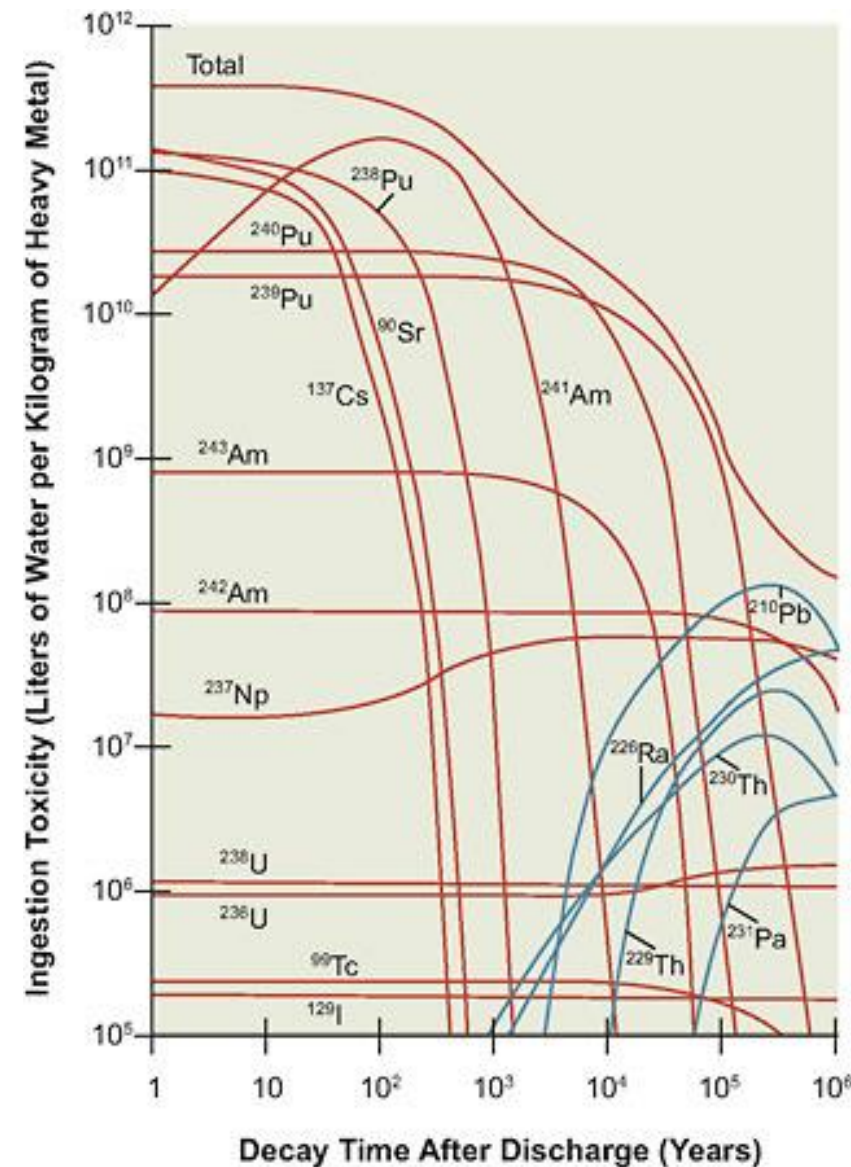
Long lived radionuclides of concern

International consensus is the application of the multi-barrier concept in radioactive waste disposal



In most European disposal concepts the waste package container is typically stainless steel and the credited lifetime is ca. 10^3 - 10^4 y

So key long lived nuclides of concern are: ^{99}Tc , ^{129}I , ^{239}Pu , ^{237}Np (plus various daughters)





Long lived radionuclides of concern

In wasteforms for higher activity wastes:

Alpha decay results in a 100 keV recoil nucleus and 5 MeV He nucleus; energy transfer is mainly by elastic scattering and ionisation processes, respectively

Beta decay results in transmutation and electron emission; energy transfer is mainly by ionisation processes (few atom displacements)

Rates of (α, n) and spontaneous fission are low and do not contribute significantly to damage

Elastic collisions from α -recoil result in atomic displacements – most important damage mechanism for crystalline ceramics

Consequently, we are most concerned with damage in ceramics for actinide immobilisation

See Figure 4
[Weber et al., J. Mater. Res., 13 \(1998\) 1434.](#)



Long lived radionuclides of concern

Crystalline ceramic wasteforms for actinide disposition typically undergo a crystalline to amorphous phase transition above ca. 1 dpa

Note that ground water will contact a radiation amorphised material after 10^3 - 10^4 y

Zirconate ceramics are highly radiation tolerant, remaining crystalline far above 10 dpa

Does the radiation amorphised ceramic material dissolve at an inherently faster rate than the crystalline parent phase?

Other effects will also be operative – e.g. volume swelling resulting in micro-cracking, which increases surface area

Here, we are concerned with the inherent dissolution rate of the material

See Figure 4
[Weber et al., J. Mater. Res., 13 \(1998\) 1434.](#)



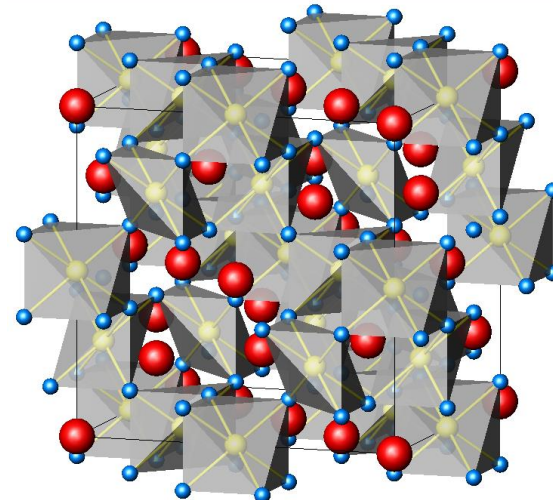
Titanate ceramics for actinide disposition

Pyrochlore : $\text{Gd}_2\text{Ti}_2\text{O}_7$

Cubic – ordered fluorite structure

Ti 6-fold co-ordinate

Gd 8-fold co-ordinate



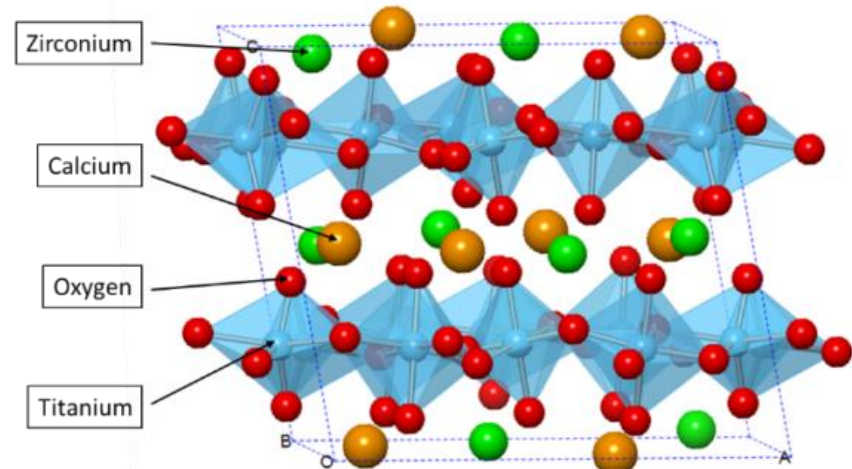
Zirconolite: $\text{CaZrTi}_2\text{O}_7$

Monoclinic – distorted ordered fluorite structure

Ti 6-fold and 5-fold co-ordinate

Ca 8-fold co-ordinate

Zr 7-fold co-ordinate





Early batch dissolution studies

Aim: to compare or measure the dissolution rates of crystalline and amorphous ceramic wasteforms

Used short lived actinide isotopes to induce damage on laboratory time scale (few years), e.g. ^{238}Pu ($t_{1/2} = 88 \text{ y}$) or ^{244}Cm ($t_{1/2} = 18 \text{ y}$)

Batch experiments:

- Monolith or powder samples
- Aqueous solution
- Teflon or other container

Key variables:

- Temperature
- Time
- Surface area / volume ratio
- pH (...radiolysis)
- Atmosphere and Eh

Analysis of solutions by ICP-OES/MS
or radiochemical methods (e.g. γ -counting)



Dissolution of $^{244}\text{Cm}-\text{Gd}_2\text{Ti}_2\text{O}_7$

Ceramic monoliths of ^{244}Cm ($t_{1/2} = 18$ y)doped $\text{Gd}_2\text{Ti}_2\text{O}_7$ co-precipitation; ca. 3 wt% XRD showed material completely amorphised after decays of $1.5 \times 10^{25} \alpha \text{ m}^{-3}$ Evidence of swelling but not micro-cracking up to decays of $2.3 \times 10^{25} \alpha \text{ m}^{-3}$

See Figure 1

Weber et al., Mater. Lett., 3 (1985) 173.

See Figure 2

Weber et al., Mater. Lett., 3 (1985) 173.



Dissolution of $^{244}\text{Cm}-\text{Gd}_2\text{Ti}_2\text{O}_7$

Dissolution experiments compared radiation amorphised and recrystallised material

- Static test in DIW, 90 °C, air, 14 d
- Monolith with SA / V = 10m^{-1}
- Teflon containers
- Post-test acid striping of containers
- Radiochemical analysis of Cm / Pu

See Table 1

[Weber et al., Mater. Lett., 3 \(1985\) 173.](#)

Apparent normalised mass loss was a factor of 20-50 greater for the amorphous vs. recrystallised material

Note decrease in pH – attributed to radiolysis of solution and radiolytic oxidation of dissolved N₂, producing HNO₃

Assumption that SA remains constant in comparison of amorphous vs. recrystallised materials - this is a critical uncertainty

Normalised release of ^{240}Pu daughter >> ^{244}Cm parent (“loosely bound”?); but 17% ^{240}Pu in initial ^{244}Cm feed.



Dissolution of ^{244}Cm -CaZrTi₂O₇

Ceramic monoliths of ^{244}Cm ($t_{1/2} = 16$ y) doped CaZrTi₂O₇ co-precipitation; ca. 3 wt% ^{244}Cm
XRD showed material completely amorphised
after decays of $2 \times 10^{25} \alpha \text{ m}^{-3}$
Evidence of swelling but not micro-cracking
up to decays of $2.3 \times 10^{25} \alpha \text{ m}^{-3}$

See Figure 1

Weber et al., J. Nucl. Mater., 138 (1986) 196.

See Figure 2

Weber et al., J. Nucl. Mater., 138 (1986) 196.



Dissolution of ^{244}Cm -CaZrTi₂O₇

Dissolution compared radiation
amorphised vs. recrystallised material

- Static test in DIW, 90 °C, air, 14 d
- Monolith with SA / V = 10m⁻¹
- Teflon containers
- Post-test acid striping of containers
- Radiochemical analysis of Cm / Pu

Apparent normalised mass loss was a factor of 10 greater for the amorphous vs. recrystallised material (Ca and Pu); but no enhanced release of Cm

Note increase in pH – solution radiolysis, would be expected to lead to pH drop; this could be buffered by Ca release?

See Table 3

Weber et al., J. Nucl. Mater., 138 (1986) 196.

Assumption that SA remains constant in comparison of amorphous vs. recrystallised materials - this is a critical uncertainty

Normalised release of ^{240}Pu daughter > ^{244}Cm parent (“loosely bound”?); but 17% ^{240}Pu in initial ^{244}Cm feed.



Dissolution of $^{244}\text{Cm}-\text{CaZrTi}_2\text{O}_7$

Recrystallisation proceeds via a rhombohedral metastable phase (not observed on amorphisation)
Rhombohedral phase thought to be stabilised by random Ca / Zr occupancy of A site
Not clear that unit cell volume has saturated (note that these are ex-situ data)
Plausible, but not certain, that recrystallised and virgin materials may be different

See Figure 10
[Weber et al., J. Nucl. Mater., 138 \(1986\) 196.](#)

See Figure 11

[Weber et al., J. Nucl. Mater., 138 \(1986\) 196.](#)



Ion beam implanted $\text{Ln}_2\text{Ti}_2\text{O}_7$

Comparative dissolution behaviour of ion beam amorphised and crystalline ceramic materials

In situ 0.6 MeV Bi^+ implantation showed critical dose for amorphisation to be well above room temperature and independent of composition

2MeV Au^{2+} implantation of $\text{Ln}_2\text{Ti}_2\text{O}_7$ pyrochlore ceramics up to ca. 5 ions nm^{-2}

TRIM simulation: implantation up to 5 ions nm^{-2} should produce an amorphised surface layer up to 350 nm thick

See Figure 1
[Begg et al., J. Nucl. Mater., 288 \(2001\) 208.](#)

See Figure 2
[Begg et al., J. Nucl. Mater., 288 \(2001\) 208.](#)



Ion beam implanted $\text{Ln}_2\text{Ti}_2\text{O}_7$

Grazing angle XRD showed expected suppression of Bragg reflections with decreasing angle - consistent with amorphisation

Intensity of Bragg reflections as a function of grazing angle modelled as a crystalline substrate covered with an amorphous surface layer

This allowed the thickness of the amorphous layer to be estimated at 340 nm, in agreement with TRIM calculation – 360 nm

Can now compare release rates from ion beam amorphised and crystalline material

See Figure 3
[Begg et al., J. Nucl. Mater., 288 \(2001\) 208.](#)

See Figure 4
[Begg et al., J. Nucl. Mater., 288 \(2001\) 208.](#)



Ion beam implanted $\text{Ln}_2\text{Ti}_2\text{O}_7$

Steady state (10 d) dissolution rates of 2

MeV Au⁺ to 3 - 5 ions nm⁻²:

- Dynamic flow through, 90 °C, 24 d, 2 ml d⁻¹
- Buffered pH 2, ICP-MS

For $\text{Gd}_2\text{Ti}_2\text{O}_7$ – initial rate of amorphous vs. crystalline material, increased by factor x10, for Gd and Ti

For $\text{Y}_2\text{Ti}_2\text{O}_7$ – initial dissolution rate increased by factor x10 for Ti, no difference for Y

Rate drop for amorphous samples due to precipitation of anatase – but only on upper face of sample.

See Figure 8

[Begg et al., J. Nucl. Mater., 288 \(2001\) 208.](#)

See Figure 9

[Begg et al., J. Nucl. Mater., 288 \(2001\) 208.](#)



Summary and conclusions – batch dissolution

Batch dissolution studies point to a factor of 10-50 increase in dissolution rate for radiation amorphised titanate ceramics

However, there are considerable uncertainties in the methodology

- Solution radiolysis effects are clearly apparent, resulting in pH excursion
- Container radiolysis were probably important (see later)
- Solution saturation likely to have occurred (no data, but see later)
- Not clear that recrystallised materials are equivalent to virgin materials
- Not clear that surface area constant through crystalline to amorphous transition

Hence need for dynamic experimental methodology to reduce (ideally eliminate) radiolysis and solution saturation effects



Recent single pass flow through studies

Aim: to accurately measure and differentiate the dissolution rates of crystalline and amorphous ceramic wasteforms

Used short lived actinide isotopes to induce damage on laboratory time scale (few years), e.g. ^{238}Pu ($t_{1/2} = 88$ y) or ^{244}Cm ($t_{1/2} = 18$ y)

SPFT experiments:

- Monolith or powder samples
- Aqueous solution
- Teflon or Ti container

Key variables:

- Temperature
- Flow rate / surface area ratio
- pH (...radiolysis)
- Atmosphere and Eh

Analysis of solutions by ICP-OES/MS
or radiochemical methods (e.g. γ -counting)

See Figure 2.3
[Strachan et al., The Status of Radiation Damage Effects, PNNL-13721 \(2001\).](#)

$$R_i = k_0 v_i e^{-E_a/RT} a_{H^+}^\eta \left[1 - \left(\frac{Q}{K} \right)^\sigma \right]$$



Ceramic compositions

Wasteform Compositions - Appendix B

[Strachan et al., The Status of Radiation Damage Effects, PNNL-13721 \(2001\).](#)



SPFT ^{238}Pu and ^{239}Pu -pyrochlore

Investigation of Pu-239 and Pu-238 pyrochlore wasteforms

Baseline composition phase assemblage:
major pyrochlore, minor brannerite and
zirconolite, trace rutile.

0.1 mass% Mo(VI) as soluble tracer for
dissolution experiments

Materials expected to be nearly fully
amorphous after 650 days and $3 \times 10^{18} \alpha/\text{g}$
at room temperature

Powder X-ray diffraction data for Pu-238
specimens confirms significant ingrowth of
amorphous phase

Brannerite reflections lost after 6 months;
rutile and zirconolite reflections persist

See Figure 3.1

[Strachan et al., The Status of Radiation Damage Effects, PNNL-13721 \(2001\).](#)

See Figure 3.14

[Strachan et al., The Status of Radiation Damage Effects, PNNL-13721 \(2001\).](#)



Dissolution of ^{238}Pu and ^{239}Pu -pyrochlore

Dissolution compared Pu-238 amorphous vs.
Pu-239 crystalline material

- Dynamic SPFT, 90 °C, N_2 , 350 d
- Buffered pH 2 only
- Flow rate of $2 \times 10^{-6} \text{ m}^3/\text{d}$; $2 \times 10^{-11} \text{ m}^3/\text{s}$
- Flow rate / SA (q/S) not stated
- Teflon containers; Pt liner for Pu-238
- ICP-OES, ICP-MS and γ -spectroscopy

Note steady state rate of dissolution achieved
after ca. 250d - plateau

Apparent dissolution rate for the Pu-238
amorphous vs. Pu-239 crystalline material: ca.
 $\times 10^1$ (Gd) - $\times 10^3$ (Pu, U)

Much larger effect than previously determined

See Figure 3.15

[Strachan et al., The Status of Radiation Damage Effects, PNNL-13721 \(2001\).](#)

See Figure 3.17

[Strachan et al., The Status of Radiation Damage Effects, PNNL-13721 \(2001\).](#)



pH dissolution dependence ^{239}Pu -pyrochlore

Steady state (250d) dissolution rates of Pu-239 material as a function of pH

- Dynamic SPFT, 90 °C, N₂, 350 d
- Buffered pH 2 – 11
- Flow rate of $2 \times 10^{-6} \text{ m}^3/\text{d}$; $2 \times 10^{-11} \text{ m}^3/\text{s}$
- Flow rate / SA (q/S) not stated
- Teflon containers
- ICP-OES, ICP-MS and γ -spectroscopy

Dissolution is incongruent – enhanced Ca release due to ion exchange at low pH

Low release of Ca and Mo at pH 2 attributed to solubility limiting phase (Ca) and sorption to precipitated rutile (Mo)

Dissolution rate relatively insensitive to pH, factor of x10 over range

See Figure 3.16

Strachan et al., The Status of Radiation Damage Effects, PNNL-13721 (2001).



Modification of SPFT approach

Factor of x10 – x 1000 increase in dissolution rate for Pu-238 vs. Pu-239 samples was much greater than expected

SPFT experiments with Pu-238 samples utilised Pt liner to prevent radiolysis of Teflon

However, Pu-238 leachates contained 10-100 ppm of fluoride vs. no detectable fluoride concentration in Pu-239 leachates

Potential for Teflon radiolysis to contribute to higher release rate of Pu-238 materials

Also concern that solution radiolysis may be important for Pu-238 expt – flow rate too slow
SPFT apparatus adapted with smaller titanium vessels – eliminate radiolysis and permit higher flow rates

See Figure 2.3
[Strachan et al., The Status of Radiation Damage Effects, PNNL-13721 \(2001\).](#)



q/S dependence of ^{239}Pu -pyrochlore

Steady state (10 d) dissolution rates of Pu-239 pyrochlore and zirconolite:

- Dynamic SPFT, 90 °C, N_2 , 10 d
- Buffered pH 2
- Titanium vessels (smaller volume)
- ICP-OES, ICP-MS and γ -spectroscopy

Steady state forward dissolution rates are ca. $10^{-2} - 10^{-3} \text{ g m}^{-2} \text{ d}^{-1}$

Previous study of Pu-239 pyrochlore ceramics afforded maximum dissolution rate of $10^{-4} \text{ g m}^{-2} \text{ d}^{-1}$

Previous experiments on cusp of forward rate regime (Log q/S too small)

For Pu-238 experiments: $-8 < \text{Log q/S} < -9$

See Figure 3.1

[Icehower et al., Dissolution Kinetics of Titanate-Based Ceramic Waste Forms: Results from Single-Pass Flow Tests on Radiation Damaged Specimens, PNNL-14252 \(2003\).](#)

See Figure 3.2

[Icehower et al., Dissolution Kinetics of Titanate-Based Ceramic Waste Forms: Results from Single-Pass Flow Tests on Radiation Damaged Specimens, PNNL-14252 \(2003\).](#)



Dissolution of ^{238}Pu -pyrochlore

Steady state (10 d) dissolution rates of Pu-238 pyrochlore and zirconolite; amorphous and recrystallised (i.e. identical composition):

- Dynamic SPFT, 85 °C, N_2 , 10 d
- Buffered pH 2
- Range of flow rate / SA: $-8 < \log q/\text{S} < -9$
- Titanium vessels (smaller volume)
- ICP-OES, ICP-MS and γ -spectroscopy

Steady state forward dissolution rates are ca.
 $10^{-2} - 10^{-3} \text{ g m}^{-2} \text{ d}^{-1}$

Gd most reliable indicator of dissolution

Hence – dissolution rates are not significantly different between Pu-239, Pu-238(cr) and Pu-238(am) specimens.

See Figure 3.3

[Icehower et al., Dissolution Kinetics of Titanate-Based Ceramic Waste Forms: Results from Single-Pass Flow Tests on Radiation Damaged Specimens, PNNL-14252 \(2003\).](#)

See Figure 3.4

[Icehower et al., Dissolution Kinetics of Titanate-Based Ceramic Waste Forms: Results from Single-Pass Flow Tests on Radiation Damaged Specimens, PNNL-14252 \(2003\).](#)



Ti solubility for ^{239}Pu -pyrochlore

Ti concentrations were observed to be independent of q/S in contrast to other elements in Pu-239 experiments

Data are shown for pH 2 – in all samples the Ti concentration is just above the solubility limit for TiO_2 at 100°C – anatase

Solubility not expected to be strongly dependent on temperature in range 90-100°C

Hence even under very forcing conditions at pH 2, solutions are likely to be (just) saturated with respect to TiO_2 - anatase

See Figure 3.5

[Icehower et al., Dissolution Kinetics of Titanate-Based Ceramic Waste Forms: Results from Single-Pass Flow Tests on Radiation Damaged Specimens, PNNL-14252 \(2003\).](#)



Summary and conclusions – SPFT dissolution

SPFT dissolution studies suggest no significant dissolution rate for radiation amorphised titanate ceramics

Very significant efforts to reduce uncertainties in the methodology

- Titanium construction – eliminates container radiolysis
- Buffered pH – no pH excursion
- High solution flow rate – radiolysis products removed, far from saturation
- Surface area / flow rate constant – eliminates error in normalised release

These experiments access only the inherent materials dissolution rate independent of solution radiolysis by maintaining far from saturation

This is the most reliable insight we have to date



Overall summary and conclusions

Dissolution experiments with ceramic wasteforms are challenging

- Very low solubility and dissolution rates, even at pH 2
- Batch dissolution experiments: simple but prone to solution saturation effects
- SPFT experiments: difficult to do and low dissolved concentrations

Addition of ^{238}Pu or ^{244}Cm increases the level of challenge

- Highly active, require glove box handling
- Container and solution radiolysis can be problematic, except at high q/S

To conclude we can say

The most sophisticated studies, taking stringent steps to eliminate solution radiolysis, show that the dissolution rates of crystalline and amorphised materials are not significantly different – at least within the margin of composite uncertainty (a factor of x10?)

Experiments which do not exclude solution radiolysis and saturation effects typically show a 10 – 100 fold increase in dissolution rate for amorphous vs. crystalline materials